

Enhanced Superconductivity by Electron Renormalization of a Directly Observed Brout-Visscher Local Phonon: Re in $\text{Mo}_{1-x}\text{Re}_x$

Danny P. Shum, A. Bevolo, J. L. Staudenmann, and E. L. Wolf^(a)

Ames Laboratory—U.S. Department of Energy and Department of Physics, Iowa State University, Ames, Iowa 50011

(Received 9 June 1986)

Tunneling reveals a ~ 14 -meV resonance mode of Re in $\text{Mo}_{1-x}\text{Re}_x$, $0.2 < x < 0.4$, which contributes strongly to $\alpha^2F(\omega)$ and to strong coupling, $2\Delta/kT_c - 3.53 = \delta > 0$. The anomalous softening and width of the resonance mode are consistent with the standard theory of phonon renormalization by the electron gas. These unexpected results explain the low- $N(0)$, high- T_c behavior of $\text{Mo}_{0.6}\text{Re}_{0.4}$ and possible Nb_3Ge .

PACS numbers: 74.50.+r, 63.20.Kr, 63.20.Pw, 74.70.-b

The effect of a mass defect on the vibrational spectrum $g(\omega)$ of a perfect crystal is simply described in two limits. A light mass induces a localized mode at ω_l , above the cutoff of the pure crystal. For a heavy mass, Brout and Visscher¹ predicted a lower frequency in-band resonance at ω_r . This vibration, whose amplitude is sharply peaked and 180° out of phase with the host at ω_r in the case $(m' - m)/m = \varepsilon \geq 1$, resembles a spatially localized optical mode. Because ω_r lies in the allowed band, one expects (localized-) phonon decays and a lifetime width, ω_d . The mean square vibration amplitude at frequency ω is^{1,2}

$$I(\omega) = R(\omega)g(\omega) = g(\omega) \left[\left(1 + \varepsilon \omega^2 \int \frac{g(\omega') d\omega'}{\omega^2 - \omega'^2} \right)^2 + \left(\frac{\pi}{2} g(\omega) \varepsilon \omega \right)^2 \right]^{-1}. \quad (1)$$

The resonance frequency ω_r is determined by the vanishing of the first term in the square brackets.

The existence of such resonance modes in metals has been inferred from inelastic neutron scattering.^{1,2} Systems studied include Cu:Au,³ Cr:W,⁴ and, in less detail, Mo:Re, with $m'/m = 1.94$,⁵ where $\omega_r = 3.5$ THz was reported at 15 at. % Re.

Recently, Yu and Anderson⁶ discussed electron-phonon coupling and superconductivity in high- T_c A15 metals modeled by a "local phonon" (vibration of a single atom) coupled to the Fermi gas. Their paper also presents a simplification of the usual Migdal-type theory suitable for our work. In this approximation of "spinless electrons" or Tomonaga bosons, the dispersion of the electrons is treated in a linear approximation.

The Re vibrational mode in $\text{Mo}_{1-x}\text{Re}_x$ particularly resembles this situation.⁶ The assumption of an atom whose motion is especially susceptible to screening is suggested by the large amplitude at the resonant frequency. For Re in Mo, calculation of $R(\omega_r)$ from Eq. (1) predicts a mean square amplitude (at $\omega = \omega_r$) 7 times that of the host at the same frequency. The observed peak increases, broadens, and shifts to lower energy (softens), all of which fit the picture of electron renormalization.

In superconductors, where tunneling spectroscopy can directly determine $\alpha^2F(\omega)$, several local modes, including Pb:In⁷ and Pd:D,⁸ have been observed. Surprisingly, there has apparently been no previous observation of a resonance mode by tunneling.

The T_c in bcc $\text{Mo}_{1-x}\text{Re}_x$ ^{9,10} rises from 0.92 K at $x = 0$ to about 12.3 K at $x = 0.4$ (hatched, in Fig. 1).

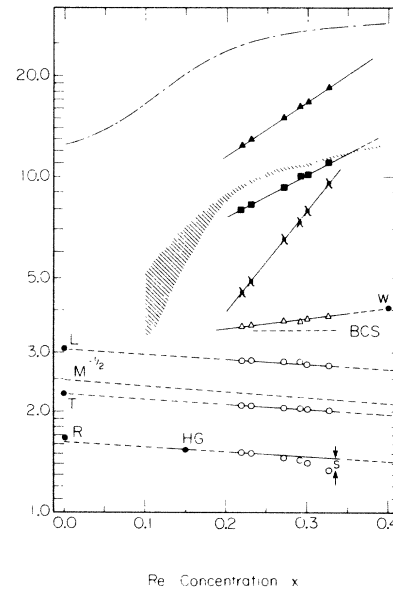


FIG. 1. Dash-dotted line: $30N(0)$, in $\text{eV}^{-1}\cdot\text{atom}^{-1}$, Ref. 10; closed triangles: $10\Delta_{\text{MoRe}}$, in meV; hatched: $t_c(x)$, in K, from Refs. 9 and 10; closed squares: gap-opening t_c , in K; lambda symbols: $10\lambda_R$ (see text); open triangles: $2\Delta/kT_c$; W: point obtained from Ref. 11; open circles: (phonon energy) $\times \frac{1}{10}$, in meV; L, T, R: (longitudinal, transverse, and R-phonon energies) $\times \frac{1}{10}$, in meV, for $x = 0$ from Fig. 2(b), and Ref. 12; $M^{-1/2}$: calculated dependence $1/M_{\text{av}}(x)^{1/2}$; HG: (R -peak energy) $\times \frac{1}{10}$ (meV) from Ref. 5; S: additional shift of peak.

The discrepancies of up to 2 K may represent different states of anneal of bulk specimens. The T_c values at electron/atom ratio $e/a=6.4$ (the second Matthias T_c peak) are similar to those in the first peak at $e/a=4.7$ ($\text{Nb}_{0.75}\text{Zr}_{0.25}$), but the density of states $N(0)$ (dash-dotted line, from Ref. 10) peaks at about $1/eV \cdot \text{atom}$, about $\frac{1}{4}$ that at $e/a=4.7$.¹⁰ The reason for the comparable T_c with reduced $N(0)$ is not clear, because no $\alpha^2F(\omega)$ results have been reported for any crystalline elements or alloys near $e/a=6.4$.

We prepared tunnel junctions on MoRe films dc sputtered at 500–700 Å/min from Mo and Re disks onto sapphire substrates at about 900°C by use of oxidized 40-Å Al film barriers and Pb counterelectrodes. Diffractometer measurements confirmed the A2 (bcc) crystalline phase of MoRe with about 500-Å grains. Resistance ratios were 1.7 to 2.8, and x was determined by electron microprobe under individual junctions. Lattice parameters $a_0=3.134$ and 3.1265 Å, respectively, at x values of 0.225 and 0.335 agree to 1% in x with published bcc a_0 vs x data.^{13,14}

Tunneling I - V measurements of the gap Δ and T_c of individual junctions determined from dV/dI spectra are summarized in Fig. 1. The T_c 's of our films are 0.2 to 1 K lower than for bulk samples.^{9,10} In view of the sensitivity to preparation of bulk samples, we attribute this small, $\cong 2\%$ – 10% reduction to the smaller grain size. The gap x and T_c measurements, plus Eliashberg inversions, characterize the MoRe in each junction. The values of $2\Delta/kT_c$ of six junctions ($x=0.22$ to 0.33) are shown in Fig. 1. The values are seen to rise above the BCS ratio (3.53, dashed line in Fig. 1).

In tunneling measurements at 1.4 K with the Pb electrode normal, three phonon peaks were observed directly in the dV/dI and d^2V/dI^2 curves. We determined $\alpha^2F(\omega)$ with a modified McMillan-Rowell method.¹⁵ The rms deviations between the measured T_c 's and calculated T_c 's from the inversions (not shown) average over the six junctions to 0.43 K or about 5%.

The $\alpha^2F(\omega)$ functions [Fig. 2(a)] all show an anomalous low-energy (R) peak, in addition to the Mo-derived transverse (T) and longitudinal (L) phonon peaks. For comparison, bcc $\text{Nb}_{0.75}\text{Zr}_{0.25}$ shows only two broadened peaks.^{16,17} While the $\alpha^2F(\omega)$ functions show some noise, the weights and centroids of the peaks are reliable, and this is confirmed by the systematic behavior.

Results of a simple model of the anomalous R peak are shown in Fig. 2(b). The dotted curve is the pure Mo $\alpha^2F(\omega)$ determined by point-contact spectroscopy.¹² [This spectrum was chosen rather than an $\alpha^2F(\omega)$ based on a neutron scattering $F(\omega)$ because it is a *direct* measurement, and predicts our results slightly more accurately than the calculated $\alpha^2F(\omega)$ of Pinski, Allen, and Butler.¹⁸] We take this¹² as $g(\omega)$, assuming constant $e-p$ coupling α^2 , and calculate $I(\omega)=r(\omega)g(\omega)$ from Eq.

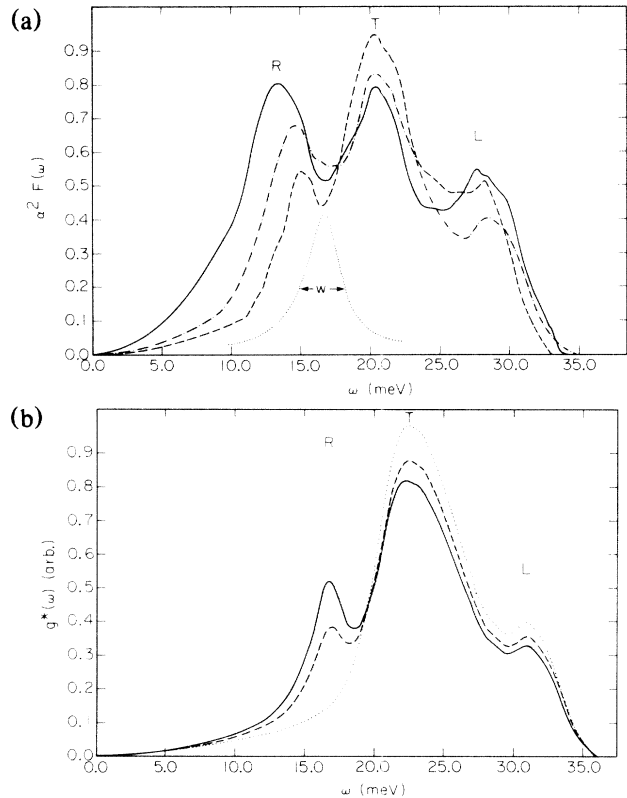


FIG. 2. (a) $\alpha^2F(\omega)$ functions measured at $x=0.33$ (solid line), $x=0.29$ (dash-dotted line), and $x=0.22$ (dashed line). Dotted inset at 16.8 meV shows $I(\omega)$ for $x=0$ calculated from Eq. (1). (b) Dotted curve, pure Mo ($x=0$) point-contact spectrum (Ref. 12). Dashed and solid curves, respectively, model $g^*(\omega)=\alpha^2F(\omega)$ (constant α^2) at $x=0.22$ and $x=0.33$, by the addition of resonance mode $I(\omega)$ to pure Mo spectrum, neglecting $M_{av}^{-1/2}$ softening.

(1). The calculated $I(\omega)$ [Fig. 2(a)] peaks at 16.8 meV. This agrees with 16.2 meV obtained (Fig. 1, lower-most curve R) by extrapolation to $x=0$ of our data (open circles) plus the value¹⁹ 15.4 meV at $x=0.15$.⁵ This extrapolation matches those (curves T and L in Fig. 1) connecting our T and L peaks to their $x=0$ limits (solid circles). For comparison, $(M_{av})^{-1/2}$ is shown dashed, and evidently can be taken as a straight line. Hence, the force constants for the Mo-derived peaks do not change much up to $x=0.35$. For the R peak additional softening S is evident.

The predicted $x=0$ line shape $I(\omega)$ is shown in Fig. 2 at 16.8 meV. Its full width is $w_d=3.15$ meV, close to the 3.2 meV estimated from Ref. 5 at $x=0.15$. This width also approximates that of the R mode in the $\alpha^2F(\omega)$ for $x=0.225$. The dashed and solid curves [modeling $g^*(\omega)=\alpha^2F(\omega)$ at $x=0.225$ and $x=0.335$] in Fig. 2(b) are obtained by addition of $I(\omega)$ and $g(\omega)$, respectively, in ratio of weights $x/(1-x)$. This neglects changes of the host spectrum with alloying and interac-

tions between Re atoms, and places all Re spectral weight in the resonance mode. Apart from our neglect of the $(M_{av})^{-1/2}$ softening, it predicts the $x=0.225$ $\alpha^2F(\omega)$ [Fig. 2(a)] reasonably well, but underestimates the strength of the R peak. This implies that the e - p coupling α^2 of the R peak exceeds that of the Mo-derived peaks. With increasing x , the R peak becomes increasingly stronger, broader, and lower in energy than the constant coupling model predicts. We conclude that the anomalous R peak at $x=0.225$ sample is the Re resonance mode, and now consider its enhancement and shift S with x , and the relation of these to the onset of strong-coupling superconductivity. The observed Δ 's and ratios $2\Delta/kT_c$ are plotted (solid triangles and open triangles, respectively) in the upper portion of Fig. 1. Note that $2\Delta/kT_c$ extrapolates to about 4.1 at $x=0.4$, which agrees with a recent report.¹¹ In addition, we have plotted (lambda symbols, Fig. 1) λ_R , the contribution to the electron-phonon coupling constant $\lambda = 2 \int_0^\infty \alpha^2 F(\omega) \times \omega^{-1} d\omega$ from the low-energy peak.²⁰ The λ_R points are seen to increase in step with $2\Delta/kT_c$.

A conventional measure of strong coupling (SC) is the deviation of $2\Delta/kT_c$ from its BCS value, namely, $\delta^{SC} \equiv 2\Delta/kT_c - 3.53$. In Fig. 3 δ^{SC} (open squares) rises more quickly than linearly versus λ_R . The dashed line is $1.26 \times \delta_{th}^{SC}$:

$$\delta_{th}^{SC} = 8.83 \frac{\lambda_R (\Delta/\omega_r)^2 \ln(\omega_r/\Delta)}{\lambda - \mu^* (1 + \lambda_R \ln 2)} \quad (2)$$

δ_{th}^{SC} , derived by Belogolovskii, Galka, and Svistunov,²¹ estimates the contribution to δ^{SC} from the R peak. Thus, we attribute about $\frac{4}{5}$ of the strong coupling δ^{SC} to

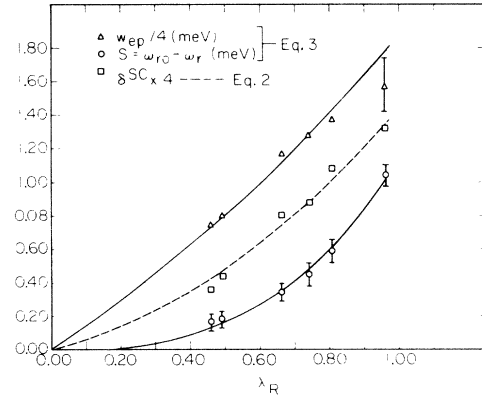


FIG. 3. Strong-coupling parameter δ^{SC} [squares, experiment; dashed line, 1.26 times Eq. (2)]; shift S (circles); and e - p width w_{ep} (triangles) of the R peak [solid curves from Eq. (3) with $a=0.245$ and $b=14.77$ meV] vs resonance mode strength λ_R .

the resonance mode.

The renormalization shift S (circles) and *electron-phonon* width w_{ep} ²² (Fig. 3, triangles) increase approximately quadratically and linearly, respectively, as functions of λ_R . While the shifts S can be directly and quite accurately determined from the displacements of the centroids of peaks in $\alpha^2F(\omega)$, the corresponding *electron-phonon* lifetime widths w_{ep} (distinct from w_d , which does not depend on e - p coupling) are less precise, as the local mode decay width w_d must be subtracted.²² The close connection between δ_{SC} and S is indicated in Fig. 3 by their similar dependences on λ_R . We have used the theory of phonon renormalization as simplified in Ref. 6 to obtain the solid curves in Fig. 3. The functions

$$S = \omega_{r0} - \omega_r = \omega_{r0} - [(\omega_{r0}^2 - b^2 a \lambda_R)(1 - a \lambda_R) - (\frac{1}{2} \pi b a \lambda_R)^2]^{1/2} / (1 - a \lambda_R), \quad (3a)$$

$$w_{ep} = \pi b a \lambda_R / 2(1 - a \lambda_R) \quad (3b)$$

[Eqs. (8) and (7), respectively, of Ref. 6] represent the real and imaginary parts of the local-phonon-Tomona-ga-boson self-energy. The values, $a=0.245$ and $b=14.77$ meV, were adjusted to fit the shift S and, without change, were used to plot the width w_{ep} , Eq. (3b). We have identified λ_R with $\Lambda^2 = \lambda_R = 2\pi N(0)I^2 / M\omega_{r0}^2$ of Ref. 6, where I is an e - p matrix element; $b = v_F k_c$, with k_c a cutoff; and $a = \omega_{r0}^2 L / 8\pi^2 v_F^2 k_c$, with L a characteristic length and v_F the Fermi velocity. Physically reasonable values, $L=1.5 \mu\text{m}$, $v_F=3 \times 10^7$ cm/s, and $k_c \cong 10^5$ cm⁻¹, for the microscopic parameters can be chosen consistent with the fit values of a and b .

From the reasonable fit of the solid lines to the data in Fig. 3, it is clear that the onset of strong-coupling superconductivity in MoRe is related to softening S of the R peak, as δ^{SC} and S are quantitatively expressed in Fig. 3 as similar functions of the same variable, λ_R . What, in turn, is responsible for the increase of λ_R with x ?

In Ref. 6, the parameter Λ^2 , which we identify with

λ_R , is proportional to I^2 (which is presumably enhanced by the large amplitude of the defect mode) and to $N(0)$. So, in the end, the increase of $N(0)$ with x , with the added "leverage" of the large I^2 , is still responsible for the increase in δ^{SC} and S . It is presumably the same leverage that enables the system to reach 12 K at $x=0.4$ with $N(0)$ only $\frac{1}{4}$ that of $\text{Nb}_{0.75}\text{Zr}_{0.25}$.

In summary, our $\alpha^2F(\omega)$ functions for MoRe, near the second Matthias $e/a=6$ peak, directly reveal for the first time a Brout-Visscher resonance mode¹ in $\alpha^2F(\omega)$. We show a quantitative connection between the strength λ_R of this mode and strong-coupling superconductivity.²¹ We suggest that the resonance-mode contribution is likely the reason for the high T_c of bcc $\text{Mo}_{0.6}\text{Re}_{0.4}$, in spite of its low $N(0)$. The softening S , width w_{ep} , and large λ_R of the Re resonance mode in MoRe are quantitatively related in Fig. 3 by e - p renormalization theory.⁶

These unexpected new results suggest tests on similar

alloys of other predictions of the Yu-Anderson model, specifically the scaling theory results which are not tested by the present work. Finally, our results lend support to the local phonon picture⁶ for $A15$ superconductors such as Nb_3Ge , where the relatively low value $N(0) = 1.2 \text{ eV}^{-1} \cdot \text{atom}^{-1}$ has been a puzzle at $T_c = 22 \text{ K}$, and where softening of specific phonons²³ has also been seen in tunneling spectra.

This work was supported by the U.S. Department of Energy Office of Basic Energy Sciences.

^(a)Permanent address: Department of Physics, Polytechnic University, Brooklyn, New York 11201.

¹R. Brout and W. Visscher, *Phys. Rev. Lett.* **9**, 54 (1962).

²P. G. Dawber and R. J. Elliott, *Proc. Roy. Soc. London, Ser. A* **273**, 222 (1963); R. J. Elliott and A. A. Maradudin, in *Inelastic Scattering of Neutrons* (International Atomic Energy Agency, Vienna, 1965), Vol. 1, p. 231.

³E. C. Svensson, B. N. Brockhouse, and J. M. Rowe, *Solid State Commun.* **3**, 245 (1965).

⁴H. B. Moller and A. R. Mackintosh, *Phys. Rev. Lett.* **15**, 623 (1965).

⁵H. G. Smith, N. Wakabayashi, and M. Mostoller, in *Superconductivity in d- and f-Band Metals*, edited by D. H. Douglass, Jr. (Plenum, New York, 1976), p. 223.

⁶C. C. Yu and P. W. Anderson, *Phys. Rev. B* **29**, 6165 (1984).

⁷J. M. Rowell, W. L. McMillan, and P. W. Anderson, *Phys. Rev. Lett.* **14**, 633 (1965).

⁸A. Eichler, H. Wuhl, and B. Stritzker, *Solid State Commun.* **17**, 213 (1975).

⁹J. K. Hulm and R. D. Blaugher, *Phys. Rev.* **123**, 1569 (1961).

¹⁰F. J. Morin and J. P. Maita, *Phys. Rev.* **129**, 1115 (1963).

¹¹J. Talvacchio, M. A. Janocko, and A. I. Braginski, *Bull. Am. Phys. Soc.* **30**, 280 (1985).

¹²J. Caro, R. Coehoorn, and D. G. de Groot, *Solid State Commun.* **39**, 267 (1981).

¹³A. Taylor, N. J. Doyle, and B. J. Kagle, *Trans. Am. Soc. Met.* **56**, 49 (1963).

¹⁴G. R. Stewart and A. L. Giorgi, *Solid State Commun.* **28**, 969 (1978).

¹⁵E. L. Wolf and G. B. Arnold, *Phys. Rep.* **91**, 32 (1982).

¹⁶E. L. Wolf and R. J. Noer, *Solid State Commun.* **30**, 391 (1979).

¹⁷F. Gompf, W. Richter, B. Scheerer, and W. Weber, *Physica (Amsterdam)* **108B**, 1337 (1981).

¹⁸F. J. Pinski, P. B. Allen, and W. H. Butler, *J. Phys. (Paris), Colloq.* **39**, C6-472 (1978); A. D. B. Woods and S. H. Chen, *Solid State Commun.* **2**, 233 (1964).

¹⁹We find that 15.4 meV is a good fit to the upper four curves in Fig. 7 of Ref. 5.

²⁰ λ_r was calculated from the portion of $\alpha^2F(\omega)$ from 0 to ω_r , by extension of the peak symmetrically above ω_r .

²¹M. A. Belogolovskii, A. A. Galkin, and V. M. Svistunov, *Fiz. Tverd. Tela*, **17**, 145 (1975) [*Sov. Phys. Solid State* **17**, 83 (1975)]. Equation (2) is an approximation to Eq. (10) of this work.

²²We have subtracted w_d according to $w_{ep} = (w^2 - w_d^2)^{1/2}$. The results are not strongly dependent on the exact procedure.

²³K. E. Kihlstrom, D. Mael, and T. H. Geballe, *Phys. Rev. B* **29**, 150 (1984).